Evidence for a Transient Peroxynitro Acid in the Reaction Catalyzed by Nitronate Monooxygenase with Propionate 3-Nitronate

2 AUTHORS:

Crystal L Smitherman
Georgia State University
4 PUBLICATIONS   **15** CITATIONS

SEE PROFILE

Giovanni Gadda
Georgia State University
**98** PUBLICATIONS   **1,616** CITATIONS

SEE PROFILE

Evidence for a Transient Peroxynitro Acid in the Reaction Catalyzed by Nitronate Monooxygenase with Propionate 3-Nitronate

Crystal Smitherman[†] and Giovanni Gadda*[,†,‡,§]

Departments of [†]Chemistry and [‡]Biology and [§]The Center for Biotechnology and Drug Design, Georgia State University, Atlanta, Georgia 30302-4098, United States

ABSTRACT: Nitronate monooxygenase is a flavin-dependent enzyme that catalyzes the denitrification of propionate 3-nitronate (P3N) and other alkyl nitronates. The enzyme was previously known as 2-nitropropane dioxygenase, until its reclassification in 2010 by the IUBMB. Physiologically, the monooxygenase from fungi protects the organism from the environmental occurrence of P3N, which shuts down the Krebs cycle by inactivating succinate dehydrogenase and fumarase. The inhibition of these enzymes yields severe neurological disorders or death. Here, we have used for the first time steady-state and rapid kinetics, viscosity and pH effects, and time-resolved absorbance spectroscopy of the enzyme in turnover with P3N and the substrate analogue ethyl nitronate (EN) to elucidate the mechanism of the reaction. A transient increase in absorbance at ~300 nm, never reported before, was seen during steady-state turnover of the enzyme with P3N and oxygen, with no concomitant changes between 400 and 600 nm. The transient species was not detected when oxygen was absent. Anaerobic reduction of the enzyme with P3N yielded anionic flavosemiquinone and was fast (e.g., ≥ 1900 s^{-1}). Steady-state kinetics demonstrated that oxygen reacts before the release of the product of P3N oxidation from the enzyme. No pH effects were seen with P3N on k_{cat}/K_m, k_{cat}/K_{oxygen}, and k_{cat}; in contrast, with EN, the k_{cat}/K_m and k_{cat} decreased with increasing pH defining two plateaus and a p$K_a \sim 8.0$. Solvent viscosity at the pH optima suggested product release as being partially controlling the overall rate of turnover with the physiological substrate and its analogue. A mechanism that satisfies the kinetic results is proposed.
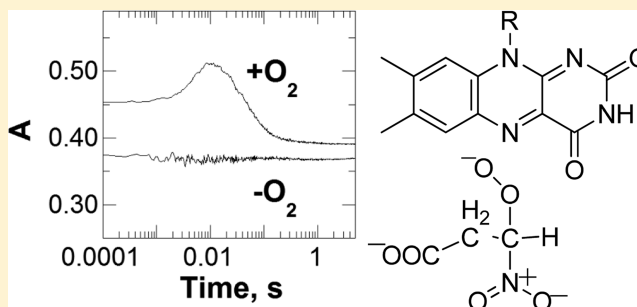
Nitronate monooxygenase (NMO, E.C. 1.13.12.16) is an FMN-dependent enzyme that catalyzes the oxidative denitrification of alkyl nitronates and the nitro acid propionate 3-nitronate (P3N) through the formation of an anionic flavosemiquinone.[1,2] The enzyme was known as 2-nitropropane dioxygenase until 2010 when the IUBMB reclassified it. NMO has been characterized biochemically and kinetically in fungi, mostly *Neurospora crassa* and, to a lesser extent, *Williopsis saturnus* var. Mrakii.[1−7] The three-dimensional structure of the enzyme from *Pseudomonas aeruginosa* is available to a resolution of 2.3 Å.[8] However, the bacterial and fungal enzymes share less than 5% sequence identity,[1] precluding structural−functional studies beyond the identification of a fully conserved histidine residue in the active site of the enzyme. In the enzyme from *N. crassa*, replacement of the conserved histidine with asparagine abolishes the ability in catalysis to utilize nitroalkanes, i.e., the conjugated acid forms of nitronates.[5] The role of the conserved histidine in the active site of the *W. saturnus* NMO is not obvious, since the enzyme can only utilize nitronates as substrates, but not nitroalkanes.[2]

The physiological role of NMO had remained elusive for decades until recent *in vivo* studies with a knockout mutant of *N. crassa* and a recombinant strain of *Escherichia coli* containing the gene encoding NMO demonstrated that the enzyme exerts a protective action from the environmental occurrence of the metabolic toxin P3N.[7] The toxicity of P3N, which is the conjugate base of 3-nitropropionic acid, arises from its ability to form an irreversible covalent adduct with succinate dehydrogenase, rendering the enzyme and the Krebs cycle completely inactive.[9−11] P3N is also a transition state analogue of fumarase.[12] The inhibition of these essential metabolic enzymes by P3N results in severe neurological disorders[13−15] and even death,[16,17] with several cases of P3N poisoning reported in livestock and hundreds of deaths in humans.[18−20] In small quantities (e.g., 20 mg/kg), P3N is routinely used to induce symptoms that mimic Huntington's disease in animal models to develop and test treatments for the disease.[21−23]

The oxidation of alkyl nitronates by NMO has been previously studied using the recombinant enzyme from *N. crassa* expressed in *E. coli* and ethyl nitronate (EN) as substrate.[3,5,6,24] Enzymatic turnover begins with the transfer of a single electron from the nitronate to the enzyme-bound FMN, yielding an anionic flavosemiquinone, as indicated by anaerobic rapid reaction data in a stopped-flow spectrophotometer.[4] The subsequent oxidation of the flavosemiquinone restores the oxidized flavin and generates a highly reactive superoxide anion, with a second-order rate constant k_{cat}/K_{oxygen} of 6×10^6 M^{-1} s^{-1} (pH 6.0 and 30 °C).[4] The EN radical and

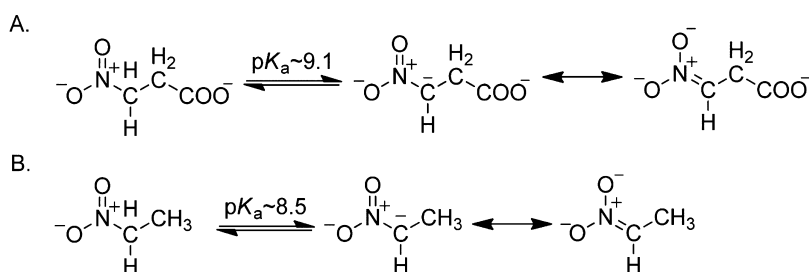**Scheme 1. (A) Ionization of 3-Nitropropionic Acid (left) To Yield P3N (right); (B) Ionization of Nitroethane (left) To Yield EN (right)**

superoxide anion have been proposed to collapse in the active site of the enzyme to form α-peroxynitroethane.[3,4] This would then decay through the effect of a nucleophile to form nitrite and acetaldehyde either on the enzyme or in solution. Evidence for the proposed radical recombination comes from the observation of an inverse α-secondary kinetic isotope effect of 0.76 on the k_{cat}/K_m with [1-^{2}H]-EN at atmospheric oxygen, which is consistent with a change in hybridization of the α-carbon atom of the EN radical from sp^2 to sp^3.[3] However, direct experimental evidence for the transient formation of α-peroxynitroethane has yet to become available. With nitroethane as substrate, enzymatic catalysis requires an extra deprotonation step catalyzed by His196 (*N. crassa* numbering), which activates the organic molecule for the subsequent one electron reaction with the flavin.[3-5] In the *N. crassa* NMO, steady-state kinetics is complicated by the partition of the EN-enzyme complex between oxidative and nonoxidative turnover due to the partial release of the EN from the enzyme active site as indicated by kinetic isotope effects, mutagenesis, and colorimetric studies.[6] Presumably the oxidation of alkyl nitronates by the *W. saturnus* NMO occurs through a similar one electron chemistry involving the organic substrate and the flavin, since the anionic flavosemiquinone is stabilized upon mixing anaerobically the enzyme with various alkyl nitronates.[2] However, no detailed mechanistic studies have been performed on the latter enzyme. With both enzymes, hydrogen peroxide is not detected during turnover with various nitronates, consistent with NMO being a monooxygenase rather than an oxidase.[1] Neither of the fungal enzymes has been characterized with the physiological substrate P3N yet. In this regard, the *W. saturnus* NMO offers itself as the best candidate for such a study because it does not catalyze the reversible conversion of the nitronate to and from the nitroalkane, being active solely with the former but not the latter.[2]

In this study, we have used steady-state kinetics, solvent viscosity, pH effects, rapid-reaction kinetics, and time-resolved absorbance spectroscopy to investigate the mechanism of NMO from *W. saturnus* with its physiological substrate P3N. The substrate analogue EN, which lacks a carboxylate group, has also been used in this study.

EXPERIMENTAL PROCEDURES

Materials. 3-Nitropropionic acid and nitroethane were from Sigma-Aldrich (St. Louis, MO). Recombinant NMO from *W. saturnus* was obtained through expression and purification methods previously described.[2] Similar to primary and secondary nitroalkanes the α-carbon of 3-nitropropionic acid has a pK$_a$ of ~9.1, allowing for a slow deprotonation with a strong base (Scheme 1).[25] P3N, the conjugate base of 3-nitropropionic acid, was therefore prepared in water by incubating the nitro compound with a 2.2 molar excess of KOH for 24 h at 4 °C. Addition of KOH was slow to avoid sample boiling and possible decomposition of P3N,[26] which was stable up to a week. EN was prepared in 100% ethanol as previously described[2] by incubating nitroethane with a 1.2 molar excess of KOH for 24 h at room temperature. The final concentration of ethanol in each assay mixture was kept constant at 1% to minimize possible effects on enzymatic activity. All other reagents were of the highest purity commercially available.

Methods. Enzymatic activity of NMO was measured by monitoring the initial rate of oxygen consumption with a computer-interfaced Oxy-32 oxygen-monitoring system (Hansatech Instruments, Inc., Norfolk, England) at 30 or 7 °C. Initial rates of reaction were calculated based on the flavin bound to the enzyme, as established spectrophotometrically. The steady-state kinetic parameters were determined by varying the concentration of oxygen and P3N (or EN), with the enzyme being gel-filtered into 10% glycerol and 50 mM potassium phosphate, pH 7.4, using a PD-10 column immediately prior to the experiment. Assay reaction mixtures were equilibrated at the desired oxygen concentrations by bubbling with an O$_2$/N$_2$ gas mixture for at least 5 min before the reaction was started with the addition of the enzyme and the substrate. When atmospheric oxygen was used with EN, the assay reaction mixtures were equilibrated with air before the reaction was started. Since the second-order rate constants for protonation of the nitronates are in the range 15-75 M^{-1} s^{-1},[27] enzymatic activity assays were initiated with the addition of the nitronate to the reaction mixture to ensure that a negligible amount of the neutral species of the nitronate was present during the time required to acquire initial rates of reaction (typically ~30 s).

The pH dependences of the steady-state kinetic parameters of the enzyme were determined as described above in the pH range between 5.5 and 11.0 in 50 mM sodium pyrophosphate at 30 °C, with the exception of pH 7.4 and 8.0 where 50 mM potassium phosphate was used. The effect of solvent viscosity on the steady-state kinetic parameters of the enzyme was determined with glycerol as viscosigen and ≥91% oxygen saturation by bubbling with an O$_2$/N$_2$ gas mixture for at least 5 min (when necessary) at pH 6.5 with P3N as substrate and pH 5.5 or pH 11.0 with EN. The relative viscosities at 30 °C were calculated from the values at 20 °C reported by Lide.[28]

Time-resolved absorbance spectroscopy of NMO in turnover was determined with a Hi-Tech SF-61 stopped-flow spectrophotometer (TgK Scientific, United Kingdom) at 30 °C, using either a xenon lamp and a photodiode array detector or a deuterium lamp and a photomultiplier detector. NMO (10 μM final) was mixed with 1 mM P3N and 0.23 mM oxygen in 50

mM potassium phosphate, pH 7.4, and allowed to turn over while acquiring 300 absorbance spectra over 1.48 s in the range from 320 to 700 nm. To identify the λ_{max} and the time course for formation and decay of the transient species observed during turnover, the experiment was repeated using the same conditions. A deuterium lamp source was used to monitor absorbance changes in the UV region and a photomultiplier detector, which allowed for acquisition of several data points in the first few milliseconds of the reaction. Single wavelength traces were acquired at 5 nm intervals from 260 to 380 nm with 8192 data points over 5 s. Using the Kinetic Studio software package of the stopped-flow instrument, the time-resolved absorbance spectra were compiled from the data points. The control experiment in the absence of oxygen was carried out in the same fashion, except the tonometer containing the enzyme was subjected to several cycles of flushing with oxygen-free argon and gas removal through applied vacuum. The syringe containing the substrate was flushed with oxygen-free argon for 20 min. Both the enzyme and substrate solutions contained a mixture of glucose (5 mM) and glucose oxidase (1 μM) as oxygen scavenger to ensure removal of trace amounts of lingering oxygen.

The reductive half-reaction of NMO with P3N was monitored using a Hi-Tech SF-61 stopped-flow spectrophotometer thermostated at 7 °C. Using a xenon lamp and photomultiplier mode, flavin reduction was established in the presence of 10% glycerol and 50 mM sodium pyrophosphate, pH 6.0, by monitoring the decrease in absorbance at 445 nm that results from the anaerobic mixing of the enzyme and substrate. An NMO solution was loaded into a tonometer and made anaerobic by a 20-cycle treatment of flushing with oxygen-free argon and gas removal by applying vacuum. The tonometer containing the anaerobic enzyme solution was mounted onto the stopped-flow instrument, which had been pretreated with an oxygen-scrubbing system composed of 5 mM glucose and 1 μM of glucose oxidase, which was also present in the tonometer. P3N was prepared in water and made anaerobic by flushing with oxygen-free argon for at least 20 min before mounting onto the stopped-flow spectrophotometer. Glucose/glucose oxidase was present in the substrate solution. After mixing in the stopped-flow spectrophotometer, the enzyme was ~10 μM and the substrate was 100 μM, ensuring pseudo-first-order kinetics. The reductive half-reaction of NMO was also examined with EN as substrate at pH 6.0 and 7 °C. The substrate was prepared in water, with a 1:1 mol equiv of KOH to avoid lingering of excess base in the solution. After mixing, the enzyme was 10 μM and the substrate between 0.8 and 42 mM. For each concentration of substrate, traces were recorded in triplicate, and the average value is reported (typically with variations ≤5%).

Data Analysis. Steady-state kinetic data were fit with KaleidaGraph (Synergy Software, Reading, PA) or Enzfitter (Biosoft, Cambridge, U.K.) software. Kinetic parameters determined with EN at atmospheric oxygen were obtained by fitting the data to the Michaelis–Menten equation for one substrate. In all cases, substrate concentrations were between 0.2 and 5 times K_m, ensuring accurate determinations of k_{cat} and k_{cat}/K_m values. When initial rates of reaction were determined at varying concentrations of P3N and oxygen, the kinetic data were fit to eq 1, which describes a steady-state kinetic mechanism in which the second substrate (oxygen) reacts before the release of the organic product of the reaction from the enzyme. k_{cat} is the first-order rate constant for the reaction

in the presence of saturating concentrations of P3N and oxygen, K_a and K_b are the Michaelis constants for P3N (A) and oxygen (B), K_{ia} is a kinetic constant that accounts for the intersecting line pattern in the double reciprocal plot, and e is the concentration of enzyme.

$$\frac{v_0}{e} = \frac{k_{cat}[A][B]}{K_a[B] + K_b[A] + [A][B] + K_{ia}K_b} \tag{1}$$

The values of eq 2 determined the corresponding pH dependencies with EN. Here, Y_H and Y_L are the limiting values at high and low pH of the parameter of interest, and K_a is the dissociation constant for relevant ionizable group(s).

$$\log Y = \log \left(\frac{Y_L + Y_H\left(\frac{10^{-pK_a}}{10^{-pH}}\right)}{1 + \left(\frac{10^{-pK_a}}{10^{-pH}}\right)} \right) \tag{2}$$

The viscosity effects on the steady-state kinetic parameters of the enzyme with P3N or EN at pH 5.5 and 6.5 were fit with eq 3 and those with EN at pH 11.0 with eq 4. The kinetic parameters measured in the absence and presence of viscosigen are k_0 and k_η, respectively, S is the degree of viscosity dependence, η_{rel} is the relative viscosity of the buffered solution, and A and B are parameters required to describe the hyperbolic behavior of the observed effect.

$$\frac{k_0}{k_\eta} = S(\eta_{rel} - 1) + 1 \tag{3}$$

$$\frac{k_0}{k_\eta} = \frac{1}{1 + A\left(\frac{\eta_{rel} - 1}{(\eta_{rel} - 1) + B}\right)} \tag{4}$$

Stopped-flow traces for the reductive half-reaction were fit with eq 5, which describes a double-exponential process. The observed first-order rate constants associated with absorbance changes of the flavin are denoted by λ_1 and λ_2, the absorbance at 445 nm at any given time is represented by A, the amplitudes of the absorbance changes associated with the two phases are denoted B and C, the absorbance at infinite time is defined as D, and time is t. The phase exhibiting the most prominent amplitude values (≥85%) is indicated as λ_1 and was plotted as a function of substrate concentration using eq 6, where k_{red} is the limiting first-order rate constant for flavin reduction at saturating substrate concentrations, K_d is the apparent dissociation constant for substrate binding, and S is the concentration of the substrate.

$$A = Be^{(-\lambda_1 t)} + Ce^{(-\lambda_2 t)} + D \tag{5}$$

$$\lambda_1 = \frac{k_{red}S}{K_d + S} \tag{6}$$

■ RESULTS

Time-Resolved Absorbance Spectroscopy of NMO in Turnover. As a first step toward the characterization of the *W. saturnus* NMO reaction with its physiological substrate P3N, time-resolved UV–vis absorbance spectra of the enzyme in turnover were monitored between 320 and 700 nm. The enzyme (10 μM) was allowed to turn over with 1 mM P3N and 0.23 mM oxygen. Data were acquired in a stopped-flow spectrophotometer equipped with a photodiode array detector

at pH 7.4 and 30 °C. After an immediate decrease in absorbance at 445 nm from 0.137 to 0.040, occurring in the mixing time of the instrument (i.e., 2.2 ms), the enzyme was primarily present as an anionic flavosemiquinone during the first 8 ms in which the steady-state persisted (Figure 1A,B). A progressive decrease of absorbance at 445 nm occurred over longer times (Figure 1A–C), yielding a final absorbance spectrum with maxima at 365 and 483 nm (Figure 1D). Thus, the enzyme-bound flavin was reduced to the anionic flavosemiquinone upon complete depletion of oxygen from the reaction mixture. Based on the molar absorption of the
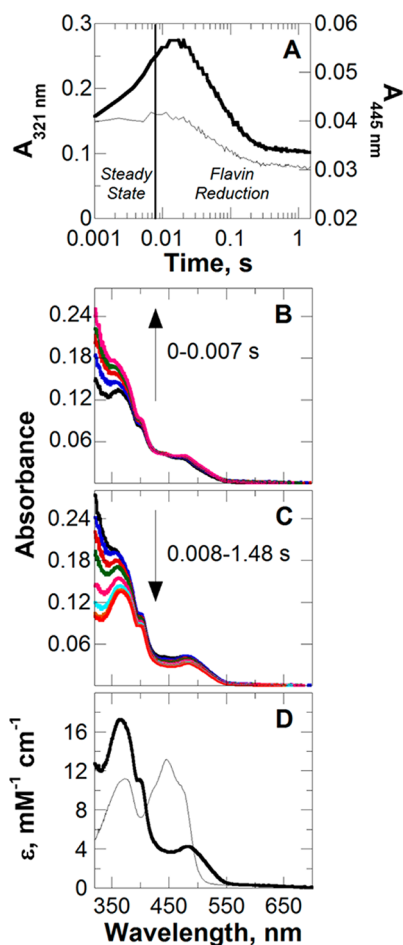
oxidized flavin in the resting state,[2] the extinction coefficient of the anionic flavosemiquinone was calculated to be 17 300 $M^{-1} cm^{-1}$ at 365 nm (Figure 1D). Interestingly, a transient increase in absorbance at 321 nm occurred within the first few milliseconds of reaction, while the enzyme was turning over with the flavin in steady state, before decreasing at longer times (Figure 1A). This suggested the formation and decay of a reaction intermediate not involving the flavin cofactor.

To determine the absorbance maximum of the transient species observed during turnover of NMO with P3N, the experiment was repeated using a monochromator and a photomultiplier detector. Single wavelength traces were acquired every 5 nm intervals from 260 to 380 nm. The time-resolved absorbance spectra were then compiled from these data points. The analysis of the absorbance spectra acquired within the first 8 ms of reaction was conducted after subtraction of the first UV−vis absorbance spectrum acquired in the stopped-flow spectrophotometer, i.e., before any transient increase in absorbance was observed. Spectral evidence showed that the reaction intermediate had maximal absorbance at ~300 nm (Figure 2A). The time course at 300
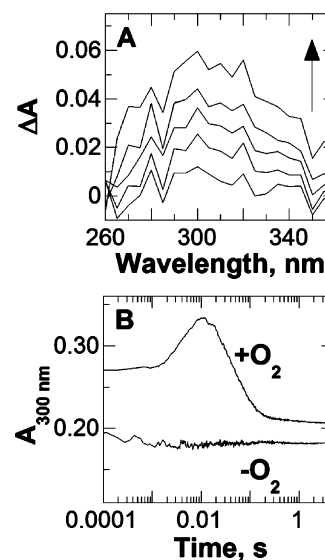

Figure 1. Time-resolved absorbance spectra of NMO (10 μM) in turnover with 1 mM P3N and 0.23 mM oxygen, in 50 mM potassium phosphate, pH 7.4 and 30 °C. The enzyme was mixed aerobically with the substrate in a stopped-flow spectrophotometer equipped with photomultiplier detector and a xenon lamp, and 300 absorbance spectra were acquired over a time of 1.48 s. All times indicated are after the end of flow, i.e., ~2.2 ms after mixing. Panel A: time course of the spectral changes at 321 nm (thick curve) and 445 nm (thin curve) associated with the absorbance spectra in panels B and C; note the log time for the x-axis; prior to mixing with substrates, the flavin absorbance at 445 nm was 0.137, as determined by mixing the resting oxidized enzyme with the reaction buffer in a 1:1 ratio. Time-resolved absorbance spectra are shown in panels B and C, where the arrows illustrate the direction of the spectral changes observed in the UV region. Panel D: comparison of the UV−vis absorbance spectra of the resting enzyme in the oxidized state (thin curve) and the semiquinone state (thick curve) obtained at 1.48 s, after complete depletion of oxygen due to enzyme turnover; note the y-axis in units of extinction coefficient rather than absorbance.

Figure 2. Time-resolved absorbance spectroscopy of NMO (10 μM) reacting with 1 mM P3N and presence and absence of 0.23 mM oxygen, in 50 mM potassium phosphate, pH 7.4 and 30 °C. The enzyme was mixed aerobically with the substrate in a stopped-flow spectrophotometer equipped with the photomultiplier detector and deuterium lamp. Traces were recorded at 5 nm intervals from 260 to 360 nm and used to compile the time-resolved absorbance spectra. All times indicated are after the end of a flow, i.e., ~2.2 ms after mixing. Panel A: spectra compiled at 2, 3, 4, 6, and 8 ms from 260 to 365 nm are shown after subtraction of the initial absorbance spectrum at 0.02 ms, yielding the difference in absorbance spectra after the initial scan is observed. Panel B: time courses of the spectral changes at 300 nm in presence and absence of oxygen; note the log time scale.

nm confirmed the preliminary data obtained at 321 nm, with transient accumulation of the reaction intermediate within the first ~8 ms of reaction and its disappearance within 0.1 s (Figure 2B). A control experiment in which the enzyme was allowed to react with P3N under the same conditions, but in the absence of oxygen, showed lack of transient changes in the trace at 300 nm (Figure 2B), and other wavelength between 260 and 360 nm (data not shown), consistent with oxygen

being required for the transient accumulation of the reaction intermediate.

Reductive Half-Reaction. The reductive half-reaction of NMO was investigated in a stopped-flow spectrophotometer at pH 6.0 and 7 °C by monitoring the loss of absorbance of the oxidized flavin at 445 nm upon mixing anaerobically the enzyme with P3N. Reactions with 100 μM P3N were completed within the mixing time of the instrument (i.e., 2.2 ms). The absorbance spectrum of the anionic flavosemiquinone was obtained at the end of the reduction (data not shown). With EN as reducing substrate, the traces at 445 nm displayed a biphasic pattern (Figure 3A), with the fast phase (λ_1)
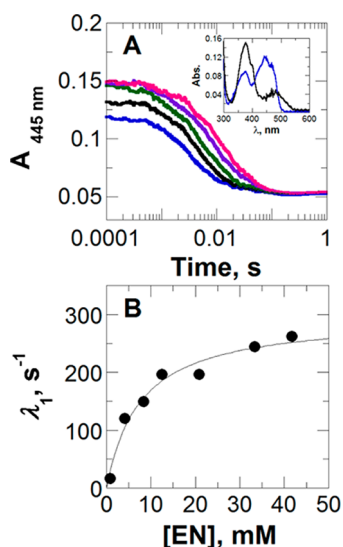

Figure 3. Anaerobic reduction of NMO with EN as substrate in 50 mM sodium pyrophosphate, pH 6.0, 7 °C, in the presence of 10% glycerol. Panel A: selected traces of flavin reduction with 50 mM (blue), 25 mM (black), 15 mM (green), 10 mM (purple), and 5 mM (pink) EN. All traces were fit with eq 5. Time indicated is after the end of flow, i.e., ~2.2 ms after mixing. Note the log time scale. Inset: absorbances of the enzyme prior to (blue) and after reacting for 1 s with 15 mM EN. Panel B: observed rate constants for flavin reduction as a function of substrate concentration. Data fit with eq 6.

accounting for the majority of the $\Delta A_{445 nm}$ (85%). The absorbance spectrum of the anionic flavosemiquinone was obtained at the end of the reduction (Figure 3A). A plot of λ_1 as a function of EN concentration yielded a hyperbola with zero y-intercept, consistent with a negligible reverse reaction of flavin reduction (Figure 3B). The first-order rate constant for flavin reduction at saturating EN (k_{red}) was calculated to be 300 $\pm$ 20 s^{-1}, whereas the apparent K_d was 8 $\pm$ 2 mM. λ_2 had an average value of 27 $\pm$ 7 s^{-1}, which was independent of EN concentration (data not shown). This was possibly due to not fully functional enzyme resulting from the preparation of the anaerobic sample or release of the organic radical product of the reaction from the enzyme active site. Since the average value of λ_2 was lower than k_{cat} (see below), the slow phase seen in the stopped-flow spectrophotometer was not associated with a kinetic step that occurred in the normal catalytic pathway of the enzyme was not investigated further.

Steady-State Kinetic Mechanism. The steady-state kinetic mechanism of NMO was determined by measuring initial rates of oxygen consumption at varying concentrations of P3N and oxygen at pH 5.5 and 30 °C. As shown in Figure 4A,
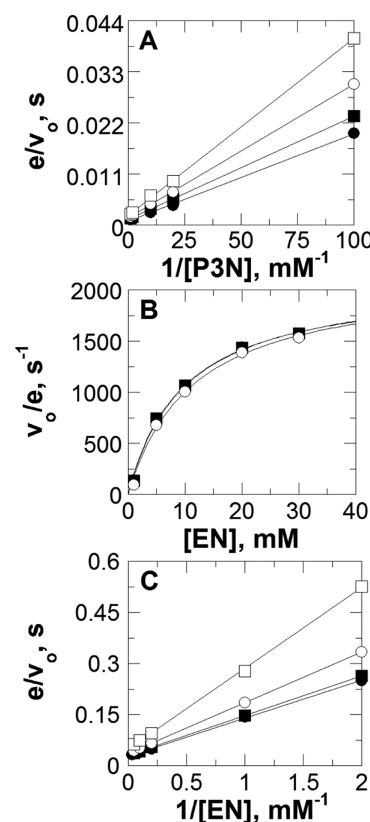

Figure 4. Steady-state kinetics of NMO with P3N or EN. Panel A: double reciprocal plot of the initial rates of reaction versus [P3N] at pH 5.5 and 30 °C with fixed oxygen concentrations of 44 μM ($\square$), 73 μM ($\bigcirc$), 115 μM ($\blacksquare$), and 145 μM ($\bullet$). Panel B: plot of the initial rates of reaction versus [EN] at pH 5.5 and 30 °C with fixed oxygen concentrations of 11 μM ($\bigcirc$), 40 μM ($\blacksquare$), and 90 μM ($\bullet$). Panel C: double reciprocal plot of the initial rates of reaction versus [EN] at pH 6.0 and 7 °C with fixed oxygen concentrations of 9 μM ($\square$), 28 μM ($\bigcirc$), 56 μM ($\blacksquare$), and 230 μM ($\bullet$), in the presence of 50 units of SOD. The lines in panels A and C represent the fit of the data with eq 1; the overlapping curves in panel B represent the fits of the data at each concentration of oxygen with the Michaelis−Menten equation for one substrate.

intersecting lines were obtained in a double reciprocal plot of the initial rate of reaction and the substrate concentration, consistent with the second substrate reacting before release of the first product of the reaction from the enzyme active site.[29] Accordingly, the data were fit best with eq 1, yielding the steady-state kinetic parameters listed in Table 1.

When EN was used as substrate for the enzyme at pH 5.5 and 30 °C, no differences in the apparent steady-state kinetic parameters were observed when oxygen was kept fixed between 11 and 90 μM (Figure 4B). This is consistent with the enzyme being fully saturated at concentrations of oxygen significantly lower than atmospheric conditions (i.e., 0.23 mM at 30 °C). Similar results were obtained with EN at pH 8.0 and 11.0 (data not shown). The overlapping saturation curves seen at different concentrations of oxygen are consistent with K_{oxygen} values not larger than 1 μM, i.e., at least 10 times smaller than the lowest concentration of oxygen used, irrespective of the pH between 5.5 and 11.0. When the steady-state kinetics with EN was determined at 7 °C, a kinetic pattern in the double reciprocal plot similar to that seen with P3N at 30 °C was obtained (Figure 4C). Unusually fast initial rates were observed at the

Table 1. Steady-State Kinetic Parameters of NMO from *W. saturnus*

substrate	pH	T (°C)	k_{cat} (s^{-1})	K_m (mM)	k_{cat}/K_m (M^{-1} s^{-1})	K_{O_2} (μM)	k_{cat}/K_{O_2} (M^{-1} s^{-1})	K_{ia} (mM)
P3N[a,d]	5.5	30	860 ± 8	0.06 ± 0.01	(1.5 ± 0.3) × 10^7	80 ± 1	(1.1 ± 0.02) × 10^7	0.31 ± 0.01
EN[a,e]	5.5	30	4100 ± 200	20 ± 2	(3.0 ± 0.3) × 10^5			
EN[b,e]	8.0	30	840 ± 10	4.0 ± 0.1	(2.0 ± 0.1) × 10^5			
EN[c,e]	11.0	30	40 ± 2	10 ± 1	(4.1 ± 0.4) × 10^3			
EN[a,d,f]	6.0	7	40 ± 1	4.0 ± 0.2	(9.6 ± 0.5) × 10^3	9 ± 1	(4.4 ± 0.3) × 10^6	4.8 ± 0.7

[a]50 mM sodium pyrophosphate. [b]50 mM potassium phosphate. [c]50 mM sodium phosphate. [d]Data were acquired at varying concentrations of substrate and oxygen and fit with eq 1 ($R^2 \geq 0.998$). [e]Data were acquired at varying concentrations of substrate and fixed oxygen concentrations of 11, 45, and 90 μM yielding overlapping saturation curves (Figure 1); kinetic parameters represent the average of the three independent measurements. [f]In the presence of 50 units of SOD.

lower temperature (data not shown). To minimize any potential radical side reaction occurring nonenzymatically[30] that might originate from EN reacting with superoxide if the latter was produced and released during turnover of the enzyme, 50 units of superoxide dismutase (SOD) were added to the reaction mixture.[30] With SOD present the initial rates were significantly lower, establishing that at low temperature superoxide was produced and released by NMO in turnover with EN. In this regard, previous studies demonstrated that SOD was not required at 30 °C with both P3N and EN.[2,7] The kinetic parameters determined with EN at low temperature are summarized in Table 1.

pH Profiles. With P3N, the effects of pH on the steady-state kinetic parameters were determined by measuring initial rates of reaction at varying concentrations of organic substrate and oxygen at 30 °C. As shown in Figure 5, there were no pH effects on the steady-state kinetic parameters between pH 5.5 and 10.5, with average values of 800 ± 100 s^{-1} for k_{cat}, (10 ± 1) × 10^6 M^{-1} s^{-1} for k_{cat}/K_m, and (15 ± 5) × 10^6 M^{-1} s^{-1} for k_{cat}/K_{oxygen}.

Because of the K_{oxygen} value being less than 1 μM (see above), pH effects with EN could only be determined at

Figure 5. Effect of pH on the steady-state kinetic parameters of NMO with P3N or EN as substrate. With P3N, initial rates of reaction were determined at varying concentrations of substrate and oxygen. Kinetic parameters were determined by using eq 1. With EN, initial rates of reaction were determined at atmospheric oxygen, yielding apparent k_{cat} and k_{cat}/K_m values that approximate well the true values due to low K_{oxygen} values (see text). All determinations were carried out at 30 °C. Panel A: k_{cat} (●) and k_{cat}/K_m (■) with P3N; k_{cat} (○) and k_{cat}/K_m (□) with EN. Data for k_{cat} and k_{cat}/K_m with EN were fit with eq 2. Panel B: pH profile of k_{cat}/K_{oxygen} with P3N.

atmospheric oxygen for the k_{cat} and k_{cat}/K_m values. The k_{cat} decreased with increasing pH from an upper limiting value of 4000 ± 400 s^{-1} to a lower limiting value of 44 ± 5 s^{-1} (Figure 5). Similarly, the k_{cat}/K_m value decreased from (3.4 ± 0.7) × 10^5 M^{-1} s^{-1} at low pH to (9 ± 2) × 10^3 M^{-1} s^{-1} at high pH (Figure 5). The pH profiles with EN defined apparent pK_a values of 7.8 ± 0.1 for k_{cat} and 7.9 ± 0.2 for k_{cat}/K_m.

Solvent Viscosity Effects. The effects of solvent viscosity on k_{cat} and k_{cat}/K_m with either P3N or EN were studied using glycerol as viscosigen to establish whether diffusion-controlled events of substrate binding and product release contributed to catalysis. These determinations were carried out at pH 6.5 with P3N and at pH 5.5 and 11.0 with EN, which correspond to the pH-independent regions identified in the pH studies (Figure 5). With P3N, the normalized k_{cat} and k_{cat}/K_m values determined at increasing relative viscosity of the solvent yielded lines with slopes of 0.34 ± 0.01 and 0.38 ± 0.03 (Figure 6). Lines with slopes of 0.48 ± 0.02 and 0.42 ± 0.04 were obtained for the k_{cat} and k_{cat}/K_m values with EN at low pH (Figure 6). Thus, similar effects were seen in k_{cat} and k_{cat}/K_m at those pH values where these kinetic parameters have maximal values. In contrast, with EN at high pH an inverse hyperbolic pattern of the normalized kinetic parameters as a function of increasing viscosity was observed (Figure 6).

■ DISCUSSION

The mechanistic study presented here provides evidence that a highly reactive peroxynitro acid is formed enzymatically during turnover of NMO with its physiological substrate, P3N. Through a single-electron transfer, P3N and NMO react to form a P3N radical species and an anionic flavosemiquinone (step B in Scheme 2). A subsequent electron transfer from the flavosemiquinone to molecular oxygen results in the oxidation of the flavin and formation of superoxide anion (step C). The two highly reactive radical species, P3N radical and superoxide, then react in the active site of the enzyme to yield 3-peroxy-3-nitro-propanoate (step D), which subsequently decays to products. Alternatively,[a] the P3N radical could react with oxygen to give a 3-peroxy-3-nitropropanoate radical (step E), which would subsequently receive an electron from the flavosemiquinone forming 3-peroxy-3-nitropropanoate (step F). Irrespective of the path, a transient 3-peroxy-3-nitro-propanoate intermediate is formed in the chemical mechanism of Scheme 2, for which evidence is presented below.

After formation of a Michaelis complex in the active site of the enzyme, NMO and P3N react through a single-electron transfer to form a P3N radical species and an anionic flavosemiquinone (step B in Scheme 2). Evidence supporting this conclusion comes from the anaerobic mixing of oxidized NMO and P3N, or its analogue EN, in a stopped-flow
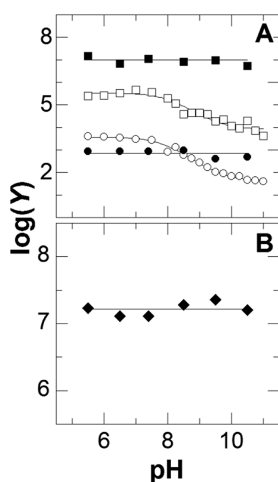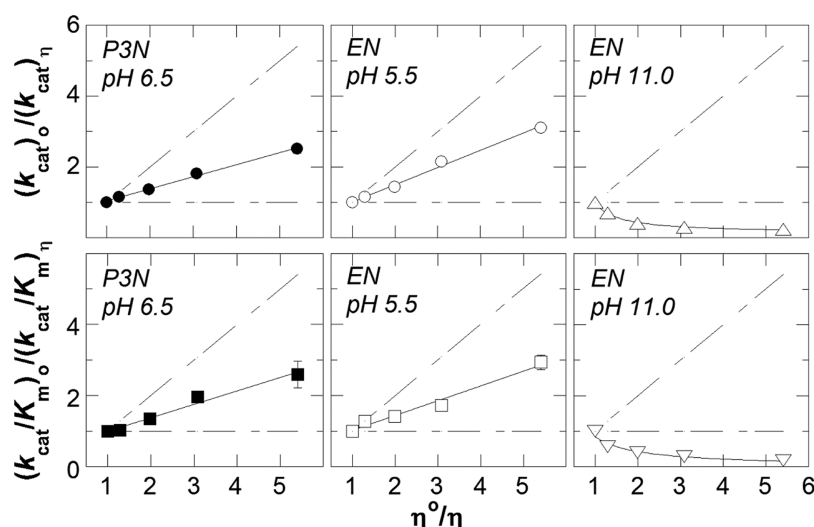
Figure 6. Effect of solvent viscosity on the steady-state kinetic parameters with P3N or EN. Initial rates were measured at 30 °C in either 50 mM sodium pyrophosphate (pH 6.5, 5.5) or sodium phosphate (pH 11.0) at varying relative viscosity of the reaction mixture. Normalized k_{cat} and k_{cat}/K_m values are shown as a function of the relative solvent viscosity. The dashed lines with a slope of +1 indicate the results expected for a fully diffusion-limited reaction. The dashed lines with a slope of 0 indicate results expected for lack of solvent viscosity effects. The values of the relative viscosities of the solvent were taken from Lide[28] and adjusted for 30 °C. Solvent viscosity data at pH 5.5 and 6.5 were fit with eq 3, and data at pH 11.0 were fit with eq 4.

Scheme 2. Minimal Chemical Mechanism of NMO with P3N and Oxygen as Substrates: (a) Michaelis Complex Formation; (b) One-Electron Flavin Reduction; (c) Oxygen Activation; (d) Formation of 3-Peroxy-3-nitropropanoate; (e) Formation of Radical 3-Peroxy-3-nitropropanoate; (f) One-Electron Transfer from the Flavosemiquinone; (g) Release of Products
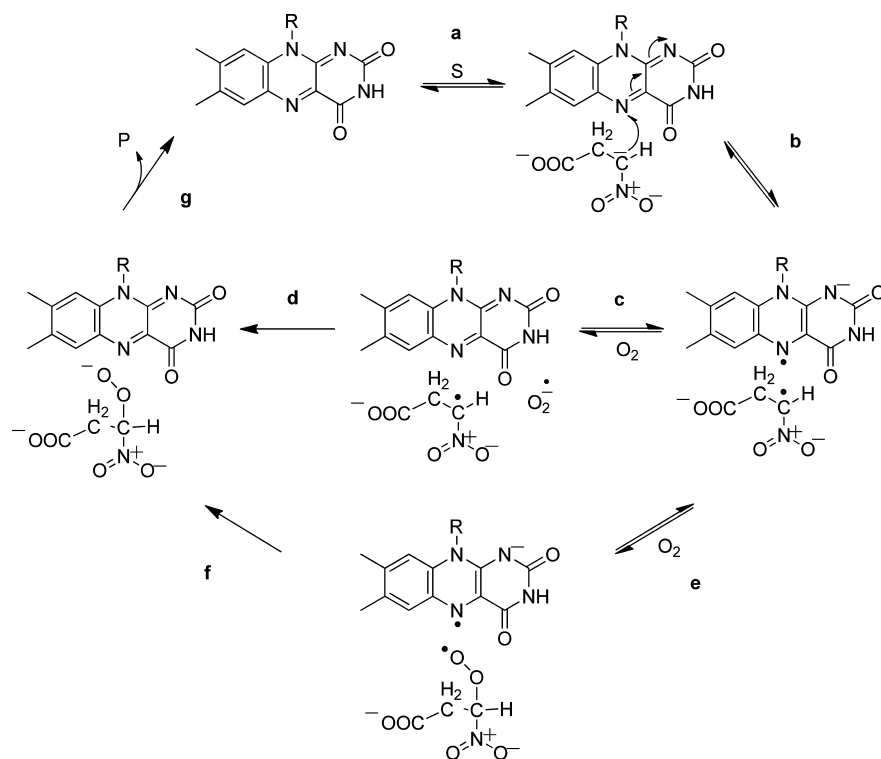
spectrophotometer. This experiment showed the rapid formation of a flavin species with λ_{max} at 365 nm, a shoulder at around 400 nm, and a less intense peak at 483 nm, which are typical of anionic flavosemiquinones.[31] The ε value of 17 300 M^{-1} cm^{-1} at 365 nm for the flavosemiquinone in NMO is comparable to those of other flavin-dependent enzymes, including D-amino acid oxidase,[31] NMO from *N. crassa*,[3] choline oxidase,[32] glycine oxidase,[33] and cholesterol oxidase,[34]

to name a few. With the physiological substrate P3N, the single-electron transfer reaction in NMO is too fast to be measured with a stopped-flow spectrophotometer, even when the temperature is lowered to 7 °C. On the basis of the mixing time of the instrument (i.e., 2.2 ms), one can estimate a rate constant for flavin reduction $\geq$1900 s^{-1} with P3N at 7 °C and pH 6.0. With EN, instead, the reduction of the flavin could be measured at low temperature, showing a limiting rate constant

of 300 s^{-1} at pH 6.0 and 7 °C. This value is 7 times larger than the turnover number of the enzyme at saturating concentrations of EN and oxygen (e.g., 40 s^{-1}), indicating that the transfer of the single-electron from the substrate to the flavin contributes minimally to the overall turnover of the enzyme at the pH optimum. Upon lowering the temperature from 30 to 7 °C, there is 100-fold decrease in the k_{cat} value with EN from 4100 s^{-1} (pH 5.5) to 40 s^{-1} (pH 6.0). It is conceivable that with P3N the k_{cat} similarly decreases from its value of 860 s^{-1} at 30 °C to ~10 s^{-1} at 7 °C. Thus, the single-electron transfer with P3N at 7 °C, with an estimated value of ≥1900 s^{-1}, does not contribute to the overall turnover of the enzyme with the physiological substrate.

Molecular oxygen is activated to superoxide through the transfer of an electron from the anionic flavosemiquinone, yielding oxidized FMN (step C in Scheme 2). The intersecting lines observed in double reciprocal plots of the initial rates of reaction as a function of P3N (or EN) concentration are consistent with oxygen reacting with the enzyme in complex with the organic product of the first electron transfer reaction, i.e., before the P3N radical is released from the enzyme active site. Further evidence in support of oxygen reacting with the flavosemiquinone comes from time-resolved absorbance spectroscopy of the enzyme turning over with P3N and oxygen and steady-state kinetics. The former experiment showed that the enzyme in turnover is primarily present as anionic flavosemiquinone, which then fully accumulates when oxygen is completely depleted from the enzyme reaction mixture. This establishes the flavosemiquinone as the species that reacts with oxygen in turnover and therefore the species that accumulates once oxygen is depleted. The effect of SOD on the steady-state kinetics with EN at low temperature showed that superoxide is produced and released from the enzyme active site during turnover. While a similar effect of SOD was not observed at 30 °C with EN or P3N irrespective of the temperature,[2,7] these results establish superoxide as a reaction intermediate that can escape from the active site at low temperature when the enzyme turns over with the substrate analogue, EN. We can speculate that the escape of superoxide from the enzyme active site may be due to an increased rigidity of the enzyme at 7 °C as compared to 30 °C.[35−37] Alternatively, if superoxide is not an obligatory intermediate, one can envision oxygen reacting directly with the P3N radical (step E in Scheme 2), followed by an electron transfer from the flavosemiquinone to form a 3-peroxy-3-nitropropanoate (step F). In this alternate mechanism the flavin would act as an electron sink that activates P3N for reaction with oxygen, instead of activating oxygen for reaction with P3N radical.

Irrespective of the flavin activating oxygen or reacting with the 3-peroxy-3-nitropropanoate radical, a 3-peroxy-3-nitropropanoate species is formed in catalysis. Evidence for the formation of 3-peroxy-3-nitropropanoate comes from the transient increase in absorbance at ~300 nm observed when the enzyme is turning over with P3N and oxygen. Lack of changes in the absorbance at 445 nm, while that at ~300 nm increases, establishes that the flavin is in steady state and is not involved in the reaction. The requirement of oxygen for the formation of 3-peroxy-3-nitropropanoate is established by the lack of spectral changes in the 260−360 nm region of the absorbance spectrum when the oxidized enzyme is mixed anaerobically with P3N. The UV absorbance spectrum of P3N in aqueous solution exhibits two maxima at 225 and 300 nm (data not shown). The increase in absorbance at ~300 nm

observed in this study is consistent with previous results in other systems demonstrating that superoxide acts as an auxochrome after reacting with other radicals, causing increases in absorbance intensity.[38−41] Alternatively, the auxochromic effect may be explained if the pK_a for the peroxy/hydroperoxy equilibrium in 3-(hydro)peroxy-3-nitropropanoate is lower than that defining the ionization of the α-carbon of P3N, yielding a reaction intermediate that is more highly ionized than the substrate.

The capture of P3N in the active site of NMO to yield a Michaelis complex competent to catalysis is very effective, as suggested by the k_{cat}/K_m value of 10^7 M^{-1} s^{-1}. High values of k_{cat}/K_m are typically seen in detoxifying enzymes involved in the elimination of reactive oxygen species, such as carbonic anhydrase, catalase, and SOD.[42−44] Besides these, only a limited number of enzymes active on organic molecules have been described to date with k_{cat}/K_m values comparable to that of NMO with P3N, namely acetyl cholinesterase, crotonase, fumarase, triose phosphate isomerase, β-lactamase, and chymotrypsin.[45−50] All of these enzymes catalyze reactions relevant to the organism as either source of energy, neurotransmitter signaling, or detoxification. In this context, the k_{cat}/K_m of 10^7 M^{-1} s^{-1} agrees well with the physiological role of NMO as an enzyme that protects fungi from the environmental occurrence of P3N, as recently established with *in vivo* studies using *N. crassa* and *E. coli.*[7]

As oftentimes observed for enzymes with k_{cat}/K_m values of 10^7−10^8 M^{-1} s^{-1},[42−51] the second-order rate constant for capture of P3N by NMO is partially controlled by the diffusion of the substrate into the active site of the enzyme. Evidence for this conclusion comes from the linear dependence of the normalized k_{cat}/K_m values on the relative viscosity of the solvent exhibiting a positive slope of 0.4. As expected for an enzyme displaying a k_{cat} with a high value of 800 s^{-1}, turnover with P3N is controlled to a significant extent by the rate of release of the product of the reaction from the active site of the enzyme. This conclusion is supported by the linear dependence with a positive slope of 0.4 of the normalized k_{cat} values as a function of the relative viscosity of the solvent. Substitution of the physiological substrate with EN, a substrate analogue lacking the carboxylate moiety, results in a 4-fold increase in k_{cat} and only a 1.3-fold increase in the solvent viscosity effect on the normalized k_{cat} values, e.g., from 0.4 with P3N to 0.5 with EN upon comparing data obtained at low pH. These data are consistent with the carboxylate group of P3N playing a major role in retaining the product in the active site of the enzyme. The carboxylate is also important for substrate binding, as demonstrated by the k_{cat}/K_m value observed at low pH with P3N being 3 orders of magnitude larger than with EN. An energetic contribution of ~17 kJ/mol can be estimated for the interaction of the carboxylate moiety of P3N toward the substrate capture by NMO. This value agrees well with that of ~15 kJ/mol previously established with the use of substrate analogues for the enzyme carboxylate in the active site of choline oxidase.[52] In that case, site-directed mutagenesis established the presence of an ionic bond between the substrate and the enzyme.[53]

The effects of pH and solvent viscosity on the k_{cat}/K_m and k_{cat} values with either P3N or EN as substrate provide the basis to explain why NMO is very proficient in capturing the organic substrate for catalysis, activating oxygen for the reaction with P3N, and a very effective catalyst in the overall turnover with P3N. The pH effects with EN demonstrate that the enzyme is 2

orders of magnitude more proficient and faster at acidic pH values than alkaline values, establishing protonation of an ionizable group as an important feature in this context. No relevant ionizations are seen in the pH profiles of k_{cat} and k_{cat}/K_m with P3N. However, the comparison of the patterns of solvent viscosity effects with EN and P3N suggests that the same enzyme species is present during turnover with the physiological substrate or EN at low pH, i.e., with a similar pattern of ionization for groups that are relevant to catalysis. Without considering the substrate carboxylate, which is likely neutralized upon substrate binding in the active site of the enzyme and does not undergo rearrangements in catalysis, all the enzyme complexes occurring in catalysis are anionic. The charge is initially on the substrate α-carbon, then on the anionic flavosemiquinone, subsequently on the superoxide, and finally on the 3-peroxy-3-nitro acid (Scheme 2). Consequently, the kinetic steps of substrate capture and oxygen activation in the mechanism of NMO, as well as the overall turnover of the enzyme, are likely enhanced by the presence of either a positive charge or a protonated group acting as a hydrogen bond donor in the active site. Studies are ongoing to determine the three-dimensional structure of the enzyme by using X-ray crystallography, which will provide a framework for future identification of the group acting as catalyst in the reaction catalyzed by fungal NMO through site-directed mutagenesis.

In conclusion, time-resolved absorbance spectroscopy of NMO in turnover with its physiological substrate P3N has allowed for the first-time detection of a proposed reaction intermediate, 3-peroxy-3-nitropropanoate. This transient intermediate is formed in the enzyme-catalyzed reaction of P3N radical and either oxygen or superoxide produced enzymatically from the reaction of oxygen with the flavosemiquinone. The flavin is instrumental for the formation of the organic radical species participating in the reaction, which is formed through a single-electron transfer from the P3N to the flavin. The study presented herein also represents the first biochemical and mechanistic characterization of NMO, which was first isolated from fungi 6 decades ago,[54] with its physiological substrate. In the GenBank, there are currently over 3000 genes annotated as NMO, or as 2-nitropropane dioxygenase as the enzyme was officially classified until 2010. Most of the products of these genes, with the exception of those from the fungi *N. crassa* and *W. saturnus*, have not been characterized biochemically. A similar physiological role in the oxidation of P3N has been established only for a single bacterial P3N monooxygenase,[55] for which limited biochemical data are available. Interestingly, bacterial and fungal NMOs appear to be only distantly related, with 20−25% amino acid similarity. This study provides therefore the groundwork for future studies that will be aimed at the characterization of other enzymes annotated as NMO with their physiological substrate, P3N.

■ AUTHOR INFORMATION

Corresponding Author

*Phone (404) 413-5537, Fax (404) 413-5505, e-mail ggadda@gsu.edu.

Notes

The authors declare no competing financial interest.

■ ABBREVIATIONS

NMO, nitronate monooxygenase; P3N, propionate 3-nitronate; EN, ethyl nitronate; SOD, superoxide dismutase; IUBMB, International Union of Biochemistry and Molecular Biology.

■ ADDITIONAL NOTE

[a]The production and release of superoxide by the enzyme in turnover with P3N at 15 °C is consistent with superoxide being a reaction intermediate that is formed in catalysis (steps C and D in Scheme 2). However, and as pointed out by one of the reviewers, the fact that superoxide leaks out of the enzyme active site during turnover under some conditions does not necessarily demonstrate that superoxide is an obligatory reaction intermediate. Thus, an alternative reaction path that leads to the formation of 3-peroxy-3-nitropropanoate through reaction of the organic radical and oxygen, followed by electron transfer from the flavosemiquinone to form the 3-peroxy-3-nitropropanoate intermediate (steps E and F in Scheme 2), cannot be ruled out. Both catalytic paths allow formation of the two species for which evidence is available in this study, i.e., the flavosemiquinone and 3-peroxy-3-nitropropanoate.

■ REFERENCES

(1) Gadda, G., and Francis, K. (2010) Nitronate monooxygenase, a model for anionic flavin semiquinone intermediates in oxidative catalysis. *Arch. Biochem. Biophys. 493*, 53−61.

(2) Mijatovic, S., and Gadda, G. (2008) Oxidation of alkyl nitronates catalyzed by 2-nitropropane dioxygenase from Hansenula mrakii. *Arch. Biochem. Biophys. 473*, 61−68.

(3) Francis, K., Russell, B., and Gadda, G. (2005) Involvement of a flavosemiquinone in the enzymatic oxidation of nitroalkanes catalyzed by 2-nitropropane dioxygenase. *J. Biol. Chem. 280*, 5195−5204.

(4) Francis, K., and Gadda, G. (2006) Probing the chemical steps of nitroalkane oxidation catalyzed by 2-nitropropane dioxygenase with solvent viscosity, pH, and substrate kinetic isotope effects. *Biochemistry 45*, 13889−13898.

(5) Francis, K., and Gadda, G. (2008) The nonoxidative conversion of nitroethane to ethylnitronate in Neurospora crassa 2-nitropropane dioxygenase is catalyzed by histidine 196. *Biochemistry 47*, 9136−9144.

(6) Francis, K., and Gadda, G. (2009) Inflated kinetic isotope effects in the branched mechanism of Neurospora crassa 2-nitropropane dioxygenase. *Biochemistry 48*, 2403−2410.

(7) Francis, K., Nishino, S. F., Spain, J. C., and Gadda, G. (2012) A novel activity for fungal nitronate monooxygenase: detoxification of the metabolic inhibitor propionate-3-nitronate. *Arch. Biochem. Biophys. 521*, 84−89.

(8) Ha, J. Y., Min, J. Y., Lee, S. K., Kim, H. S., Kim do, J., Kim, K. H., Lee, H. H., Kim, H. K., Yoon, H. J., and Suh, S. W. (2006) Crystal structure of 2-nitropropane dioxygenase complexed with FMN and substrate. Identification of the catalytic base. *J. Biol. Chem. 281*, 18660−18667.

(9) Alston, T. A., Mela, L., and Bright, H. J. (1977) 3-Nitropropionate, the toxic substance of Indigofera, is a suicide inactivator of succinate dehydrogenase. *Proc. Natl. Acad. Sci. U. S. A. 74*, 3767−3771.

(10) Coles, C. J., Edmondson, D. E., and Singer, T. P. (1979) Inactivation of succinate dehydrogenase by 3-nitropropionate. *J. Biol. Chem. 254*, 5161−5167.

(11) Huang, L. S., Sun, G., Cobessi, D., Wang, A. C., Shen, J. T., Tung, E. Y., Anderson, V. E., and Berry, E. A. (2006) 3-nitropropionic acid is a suicide inhibitor of mitochondrial respiration that, upon oxidation by complex II, forms a covalent adduct with a catalytic base

arginine in the active site of the enzyme. *J. Biol. Chem. 281*, 5965–5972.

(12) Porter, D. J., and Bright, H. J. (1980) 3-Carbanionic substrate analogues bind very tightly to fumarase and aspartase. *J. Biol. Chem. 255*, 4772–4780.

(13) Scallet, A. C., Nony, P. L., Rountree, R. L., and Binienda, Z. K. (2001) Biomarkers of 3-nitropropionic acid (3-NPA)-induced mitochondrial dysfunction as indicators of neuroprotection. *Ann. N.Y. Acad. Sci. 939*, 381–392.

(14) Ludolph, A. C., He, F., Spencer, P. S., Hammerstad, J., and Sabri, M. (1991) 3-Nitropropionic acid-exogenous animal neurotoxin and possible human striatal toxin. *Can. J. Neurol. Sci. 18*, 492–498.

(15) Pang, Z., and Geddes, J. W. (1997) Mechanisms of cell death induced by the mitochondrial toxin 3-nitropropionic acid: acute excitotoxic necrosis and delayed apoptosis. *J. Neurosci. 17*, 3064–3073.

(16) Burdock, G. A., Carabin, I. G., and Soni, M. G. (2001) Safety assessment of B-nitropropionic acid: a monograph in support of an acceptable daily intake in humans. *Food Chem. 75*, 1–27.

(17) Ming, L. (1995) Moldy sugarcane poisoning–a case report with a brief review. *J. Toxicol. Clin. Toxicol. 33*, 363–367.

(18) Hamilton, B. F., Gould, D. H., and Gustine, D. L. (2000) History of 3-nitropropionic acid, in *Mitochondrial Inhibitors and Neurodegenerative Disorders Comptemporary Neuroscience*, Humana Press, Totowa, NJ.

(19) Mathews, F. P. (1940) The toxicity of red-stemmed peavine (*Astragalus emoryanus*) for cattle, sheep, and goats. *J. Am. Vet. Med. Assoc. 97*, 125–134.

(20) Liu, X., Luo, X., and Hu, W. (1992) Studies on the epidemiology and etiology of moldy sugarcane poisoning in China. *Biomed. Environ. Sci. 5*, 161–177.

(21) Beal, M. F., Brouillet, E., Jenkins, B. G., Ferrante, R. J., Kowall, N. W., Miller, J. M., Storey, E., Srivastava, R., Rosen, B. R., and Hyman, B. T. (1993) Neurochemical and histologic characterization of striatal excitotoxic lesions produced by the mitochondrial toxin 3-nitropropionic acid. *J. Neurosci. 13*, 4181–4192.

(22) Guyot, M. C., Hantraye, P., Dolan, R., Palfi, S., Maziere, M., and Brouillet, E. (1997) Quantifiable bradykinesia, gait abnormalities and Huntington's disease-like striatal lesions in rats chronically treated with 3-nitropropionic acid. *Neuroscience 79*, 45–56.

(23) Tsang, T. M., Haselden, J. N., and Holmes, E. (2009) Metabonomic characterization of the 3-nitropropionic acid rat model of Huntington's disease. *Neurochem. Res. 34*, 1261–1271.

(24) Francis, K., and Gadda, G. (2009) Kinetic evidence for an anion binding pocket in the active site of nitronate monooxygenase. *Bioorg. Chem. 37*, 167–172.

(25) Bush, M. T., Touster, O., and Brockman, J. E. (1951) The production of beta-nitropropionic acid by a strain of Aspergillus flavus. *J. Biol. Chem. 188*, 685–693.

(26) Lewis, R. J. (1996) *Sax's Dangerous Properties of Industrial Materials*, 9th ed., Van Nostrand Reinhold, New York.

(27) Nielsen, A. T. (1969) Nitronic acids and esters, in *The Chemistry of the Nitro and Nitroso Groups* (Feuer, H., Ed.), pp 349–486, Interscience Publishers, New York.

(28) Lide, D. R. (2000) *Handbook of Chemistry and Physics*, 6th ed., CRC Press, Boca Raton, FL.

(29) Segel, I. H. (1975) *Enzyme Kinetics*, Wiley, New York.

(30) Kuo, C. F., and Fridovich, I. (1986) Free-radical chain oxidation of 2-nitropropane initiated and propagated by superoxide. *Biochem. J. 237*, 505–510.

(31) Massey, V., and Palmer, G. (1966) On the existence of spectrally distinct classes of flavoprotein semiquinones. A new method for the quantitative production of flavoprotein semiquinones. *Biochemistry 5*, 3181–3189.

(32) Ghanem, M., Fan, F., Francis, K., and Gadda, G. (2003) Spectroscopic and kinetic properties of recombinant choline oxidase from Arthrobacter globiformis. *Biochemistry 42*, 15179–15188.

(33) Job, V., Marcone, G. L., Pilone, M. S., and Pollegioni, L. (2002) Glycine oxidase from Bacillus subtilis. Characterization of a new flavoprotein. *J. Biol. Chem. 277*, 6985–6993.

(34) Gadda, G., Wels, G., Pollegioni, L., Zucchelli, S., Ambrosius, D., Pilone, M. S., and Ghisla, S. (1997) Characterization of cholesterol oxidase from Streptomyces hygroscopicus and Brevibacterium sterolicum. *Eur. J. Biochem. 250*, 369–376.

(35) Dougherty, R. C. (1998) Temperature and pressure dependence of hydrogen bond strength: A perturbation molecular orbital approach. *J. Chem. Phys. 109*, 7372–7378.

(36) Jaenicke, R. (1990) Protein structure and function at low temperatures. *Philos. Trans. R. Soc. London, B 326*, 535–551 ; discussion: 551–553.

(37) Cordier, F., and Grzesiek, S. (2002) Temperature-dependence of protein hydrogen bond properties as studied by high-resolution NMR. *J. Mol. Biol. 317*, 739–752.

(38) Takahashi, K., Numata, N., Kinoshita, N., Utoguchi, N., Mayumi, T., and Mizuno, N. (2004) Characterization of the influence of nitric oxide donors on intestinal absorption of macromolecules. *Int. J. Pharm. 286*, 89–97.

(39) Kelm, M., Dahmann, R., Wink, D., and Feelisch, M. (1997) The nitric oxide/superoxide assay. Insights into the biological chemistry of the NO/O-2. interaction. *J. Biol. Chem. 272*, 9922–9932.

(40) Bamdad, F., Wu, J., and Chen, L. (2011) Effects of enzymatic hydrolysis on molecular structure and antioxidant activity of barley hordein. *J. Cereal Sci. 54*, 20–28.

(41) Evans, J. P., Niemevz, F., Buldain, G., and de Montellano, P. O. (2008) Isoporphyrin intermediate in heme oxygenase catalysis. Oxidation of alpha-meso-phenylheme. *J. Biol. Chem. 283*, 19530–19539.

(42) Fielden, E. M., Roberts, P. B., Bray, R. C., Lowe, D. J., Mautner, G. N., Rotilio, G., and Calabrese, L. (1974) Mechanism of action of superoxide dismutase from pulse radiolysis and electron paramagnetic resonance. Evidence that only half the active sites function in catalysis. *Biochem. J. 139*, 49–60.

(43) Maehly, A. C., and Chance, B. (1954) The assay of catalases and peroxidases. *Methods Biochem. Anal. 1*, 357–424.

(44) Hasinoff, B. B. (1984) Kinetics of carbonic anhydrase catalysis in solvents of increased viscosity: a partially diffusion-controlled reaction. *Arch. Biochem. Biophys. 233*, 676–681.

(45) Quinn, D. M. (1987) Acetylcholinesterase: Enzyme structure, reaction dynamics, and virtual transition states. *Chem. Rev. 87*, 955–979.

(46) Waterson, R. M., and Hill, R. L. (1972) Enoyl coenzyme A hydratase (crotonase). Catalytic properties of crotonase and its possible regulatory role in fatty acid oxidation. *J. Biol. Chem. 247*, 5258–5265.

(47) Sweet, W. L., and Blanchard, J. S. (1990) Fumarase: viscosity dependence of the kinetic parameters. *Arch. Biochem. Biophys. 277*, 196–202.

(48) Blacklow, S. C., Raines, R. T., Lim, W. A., Zamore, P. D., and Knowles, J. R. (1988) Triosephosphate isomerase catalysis is diffusion controlled. Appendix: Analysis of triose phosphate equilibria in aqueous solution by 31P NMR. *Biochemistry 27*, 1158–1167.

(49) Christensen, H., Martin, M. T., and Waley, S. G. (1990) Beta-lactamases as fully efficient enzymes. Determination of all the rate constants in the acyl-enzyme mechanism. *Biochem. J. 266*, 853–861.

(50) Brouwer, A. C., and Kirsch, J. F. (1982) Investigation of diffusion-limited rates of chymotrypsin reactions by viscosity variation. *Biochemistry 21*, 1302–1307.

(51) Wilcox, P. E. (1970) Chymotrypsinogens-chymotrypsins. *Methods Enzymol. 19*, 64–108.

(52) Gadda, G., Powell, N. L., and Menon, P. (2004) The trimethylammonium headgroup of choline is a major determinant for substrate binding and specificity in choline oxidase. *Arch. Biochem. Biophys. 430*, 264–273.

(53) Quaye, O., Lountos, G. T., Fan, F., Orville, A. M., and Gadda, G. (2008) Role of Glu312 in binding and positioning of the substrate for the hydride transfer reaction in choline oxidase. *Biochemistry 47*, 243–256.

(54) Little, H. N. (1951) Oxidation of nitroethane by extracts from Neurospora. *J. Biol. Chem. 193*, 347–358.

(55) Nishino, S. F., Shin, K. A., Payne, R. B., and Spain, J. C. (2010) Growth of bacteria on 3-nitropropionic acid as a sole source of carbon, nitrogen, and energy. *Appl. Environ. Microbiol.* 76, 3590−3598.